PRAMANA
— journal of
physics

Vol. 85, No. 4
October 2015
pp. 713–721

Second-harmonic ion cyclotron resonance heating scenarios of Aditya tokamak plasma

ASIM KUMAR CHATTOPADHYAY*, S V KULKARNI, R SRINIVASAN and Aditya team

Institute for Plasma Research, Bhat, Gandhinagar 382 428, India
*Corresponding author. E-mail: asim@ipr.res.in

MS received 13 December 2013; revised 17 April 2014; accepted 21 August 2014
DOI: 10.1007/s12043-014-0908-1; ***e*Publication:** 2 May 2015

Abstract. Plasma heating with the fast magnetosonic waves in the ion cyclotron range of frequencies (ICRF) is one of the auxiliary heating schemes of Aditya tokamak. Numerical simulation of second-harmonic resonance heating scenarios in low-temperature, low-density Aditya plasma has been carried out for fast magnetosonic wave absorption in ICRF range, using full-wave ion cyclotron heating code TORIC combined with Fokker–Planck quasilinear solver SSFPQL and the results are explained. In such low-temperature, low-density plasma, ion absorption for second-harmonic resonance heating is less but significant amount of direct electron heating is observed.

Keywords. Second-harmonic ion cyclotron resonance heating; Aditya tokamak; fast wave; mode conversion.

PACS Nos 52.50.Qt; 52.55.Fa; 52.50.−b

1. Introduction

One of the most promising plasma heating mechanisms in the ion cyclotron (IC) range of frequencies (ICRF) is the pure second-harmonic ion cyclotron (IC) resonance interaction with plasma ions. In single species plasma second-harmonic IC resonance frequency is the only choice to interact with plasma ions, as fundamental IC resonance heating is not effective due to mismatch of the direction of wave polarization and that of the motion of ions [1]. It is to be noted that electric field of fast magnetosonic waves or fast waves in its fundamental frequency is exact circular right-hand polarized, but free ion is left-hand polarized; whereas fast wave at harmonics is elliptically polarized, and hence one can divide the electric field component perpendicular to the background magnetic field in two components: one component (E_+) rotates in the same direction as the ions and the other component (E_-) counterrotates. To the lowest order, it is the E_+ that gives rise to absorption.

The tokamak Aditya [2] plasma is a low-density, low-temperature, pure hydrogen plasma having a second-harmonic resonance layer at $\sim$6.0 cm from plasma centre and

at high field side. Direct electron heating experiment on the Aditya tokamak using fast waves (FW) in the IC frequency range has already been carried out in [3] and significant direct electron heating was observed in hydrogen plasma. Ion heating was not measured. Wave absorption in low-temperature, low-density plasma could be important, both from fundamental physics point of view as well as for application in Aditya-like tokamak. To the best of our knowledge wave absorption scenarios in such plasmas have not been studied properly so far. This paper presents numerical simulation of the wave absorption by ions and electrons and related phenomena in low-temperature and low-density Aditya plasma due to second-harmonic IC resonance heating taking the plasma parameters and experimentally estimated absorbed energy, with the full wave IC resonance heating code TORIC [4] coupled to the Fokker–Planck quasilinear solver SSFPQL [5]. It is expected that the ion temperature estimated in this work may be helpful in facilitating the development and benchmarking of charge exchange diagnostic meant for measuring ion temperature profiles, which is currently being developed for Aditya.

TORIC is a finite Larmor radius (FLR) full-wave code which solves the wave equation in general toroidal axisymmetric configurations. The wave equations are derived from Vlasov equation by expanding the electromagnetic fields in Fourier modes in toroidal and poloidal angles. A detailed description is given in [4]. The code TORIC describes wave propagation and absorption by ions at fundamental ($\omega = \Omega_{\rm ci}$) and second-harmonic ($\omega = 2\Omega_{\rm ci}$) whereas electron absorption via electron Landau damping (ELD), transit time magnetic pumping (TTMP), and their cross term absorption. It can also model ion Bernstein wave (IBW) and ion cyclotron wave (ICW) at the ion–ion resonance layer. Steady-state Fokker–Planck quasilinear (SSFPQL) code solves the steady-state surface-averaged quasilinear Fokker–Planck equation for ions heated at the fundamental and second-harmonic cyclotron frequencies and evaluate the distribution function, using the quasilinear diffusion coefficients for each magnetic surface evaluated by TORIC. The output of full-wave TORIC code, viz., magnetic surface-averaged power deposition profile is exported to SSFPQL. Once the quasilinear distribution function of the ions has been evaluated by SSFPQL, the module QLMINH helps TORIC to estimate the influence of suprathermal population on wave propagation and absorption [6]. So, TORIC and SSFPQL are interlinked. SSFPQL provides information on the distribution function, radial profiles of parallel and perpendicular energies, number of fast ions of high-energy (suprathermal) tail generated by IC resonance heating. It also provides information on the collisional exchanges between these tails and background ions and electrons.

The rest of the paper is organized as follows: Section 2 describes a brief model and mathematical description used in TORIC and SSFPQL. Section 3 is dedicated for results and discussion whereas §4 concludes the results with some comments.

2. The TORIC code and SSFPQL module

TORIC solves inhomogeneous Maxwell's equations in the presence of plasma and wave antenna

$$\vec{\nabla} \times (\vec{\nabla} \times \vec{E}) = \frac{\omega^2}{c^2}\left[\vec{E} + \frac{4\pi i}{\omega}(\vec{J}^{\rm P} + \vec{J}^{\rm A})\right], \tag{1}$$

Table 1. Antenna parameters and main plasma parameters of the shot # 20685 used in the simulation. The profiles of n and T have been approximated analytically.

Major radius	75 cm
Plasma radius	25 cm
Frequency	24.8 MHz
Antenna length	30.0 cm
Strap width	10 cm
Magnetic field	0.75 T
Toroidal current	78.5 kA
Central electron density	1.6×10^{13} cm^{-3}
Central electron temperature	0.310 keV
Central ion temperature	0.155 keV
Distance between plasma and Faraday shield	1.0 cm
Distance between plasma and antenna	3.5 cm
Distance between plasma and wall	5.8 cm
Representative toroidal wavenumber	$n_\phi = 8$
Estimated total power coupled	44×10^{-3} MW

where $\vec{J}^{\mathrm{A}}$ is the source (antenna) current and $\vec{J}^{\mathrm{P}}$ is the high-frequency (hf) plasma current. In FLR approximation, $\vec{J}^{\mathrm{P}}$ can be approximated as [4,7]

$$\vec{J}^{\mathrm{P}} = \vec{J}^{0} + \sum_{\mathrm{s}} \vec{J}_{\mathrm{s}}^{(2)}. \tag{2}$$

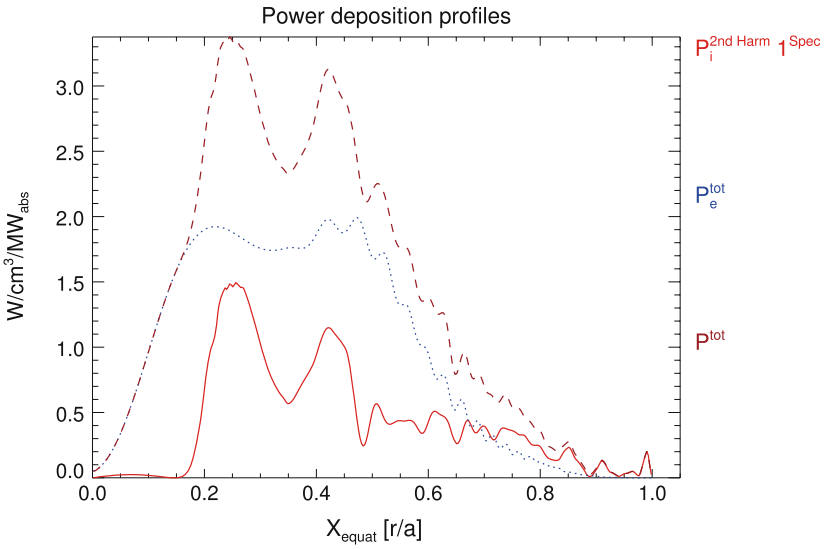

Figure 1. Radial power deposition profiles of shot #20685 evaluated by TORIC. The curve $P_{\mathrm{i}}^{2\mathrm{ndHarm}}{}_1{}^{\mathrm{Spec}}$ (solid line) shows the power deposition profile of ions due to second-harmonic heating whereas the curve $P_{\mathrm{e}}^{\mathrm{tot}}$ (dotted line) shows the total power deposition profile of electrons. The curve P^{tot} (dashed line) represents the profile of total power absorbed. The total power is normalized to 1 MW.

Summation is over all species, s. $\vec{J}^0$ denotes the zero Larmor radius current and the second term on the right-hand side of eq. (2) is the FLR current of ions and electrons. FLR expansion makes sense only when it can be stopped at second order which describes the pressure driven waves. It is extremely tedious to calculate the terms, beyond second order and in most cases they do not elucidate any physical meaning [4]. All 'diamagnetic' contributions to the hf plasma current $\vec{J}^{\mathrm{P}}$ (i.e., terms proportional to ∇n, ∇T_{i}, ∇T_{e}) have been neglected. Omitting these terms eliminates the drift branch of dispersion relation, but has a negligible influence on waves in the IC frequency range [4]. The FLR ion terms resonant at the fundamental cyclotron frequency is also omitted. These terms are always small corrections to the zero Larmor radius currents, which is also resonant at $\omega = \Omega_{\mathrm{ci}}$.

The numerical solution of the above wave equation is based on the spectral representation of the wave fields in the poloidal angle θ, and a cubic Hermite finite element in the radial variable is as follows (cubic Hermite polynomial is the basis function in finite element method) [4]:

$$\vec{E} = \sum_{m_\theta, n_\phi} \vec{E}^{m_\theta, n_\phi}(r) \mathrm{e}^{\mathrm{i}(m_\theta \theta + n_\phi \phi)}. \tag{3}$$

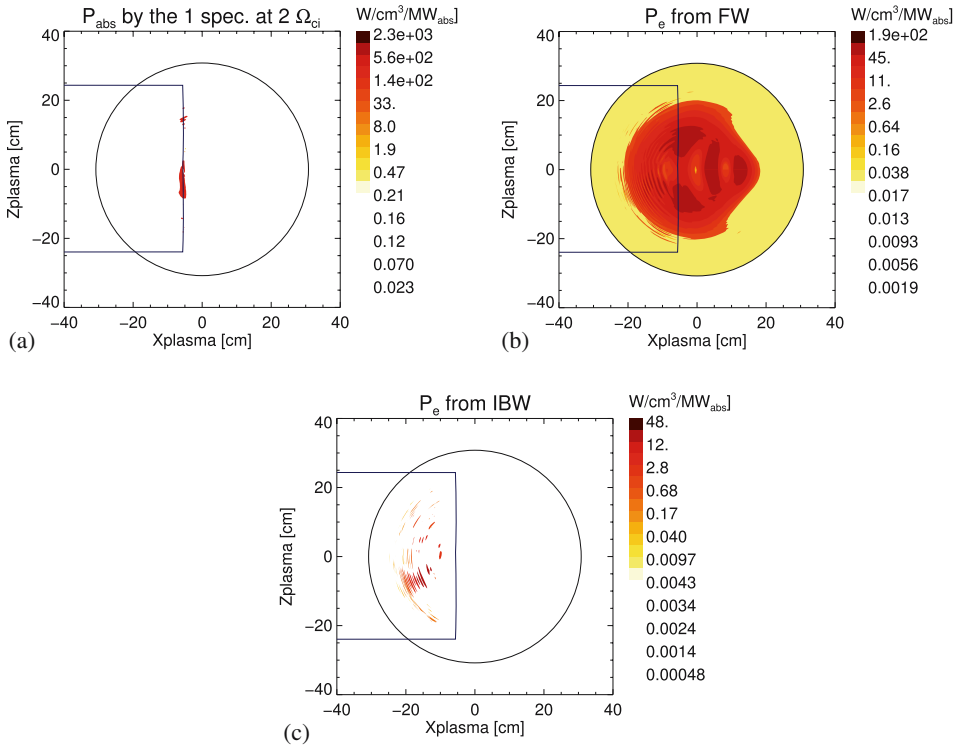

Figure 2. Power absorbed by **(a)** ions at the second-harmonic from FW, **(b)** electrons from FW, **(c)** electrons from IBW in the poloidal cross-section as evaluated by TORIC. The vertical line indicates the second-harmonic resonance layer for hydrogen ions.

A weak formulation of the wave equation is used which is done with the help of standard Galarkin's method. Suitable regulatory conditions on magnetic axis; boundary conditions at the plasma edge, Faraday shield, antenna and wall are used to solve wave equation with the finite element method. A detailed description of these boundary conditions can be found in [4].

The code SSFPQL based on the quasilinear kinetic equation is as follows:

$$\frac{\mathrm{d}F_\mathrm{i}}{\mathrm{d}t} = \left(\frac{\partial F_\mathrm{i}}{\partial t}\right)_\mathrm{QL} + \left(\frac{\partial F_\mathrm{i}}{\partial t}\right)_\mathrm{coll} + \left(\frac{\partial F_\mathrm{i}}{\partial t}\right)_\mathrm{loss}. \tag{4}$$

The term $\mathrm{d}F_\mathrm{i}/\mathrm{d}t$ on the left-hand side of the above equation is the evolution of distribution function with time whereas the first term $(\partial F_\mathrm{i}/\partial t)_\mathrm{QL}$ on the right-hand side is the quasilinear operator, the 2nd term $(\partial F_\mathrm{i}/\partial t)_\mathrm{coll}$ is the Fokker–Planck collisional operator, and the third term $(\partial F_\mathrm{i}/\partial t)_\mathrm{loss}$ is the loss term. It is to be noted that the quasilinear diffusion coefficient has a strong pitch angle, μ dependence. The code SSFPQL solves the steady-state $((\mathrm{d}F_\mathrm{i}/\mathrm{d}t) = 0)$ quasilinear kinetic equation for IC heated ions [5], neglecting the loss term.

$$0 = \left(\frac{\partial F_\mathrm{i}}{\partial t}\right)_\mathrm{QL} + \left(\frac{\partial F_\mathrm{i}}{\partial t}\right)_\mathrm{coll} + S_\mathrm{i}(v). \tag{5}$$

The isotropic source term $S_\mathrm{i}(v)$ is added to maintain different background species at different temperatures in the absence of hf wave heating.

It is to be noted that SSFPQL is based on a rather simplified model. It takes surface-averaged, uniform-plasma Kennel–Engelmann quasilinear operator [5] neglecting the effect of toroidicity on IC heating, viz., toroidal trapping, finite banana width and loss. It also considers that the collisional operator is linearized, assuming that the fast ion distribution function reaches steady state by losing energy on the background ions and electrons. For these assumptions SSFPQL is not the proper substitute of sophisticated Fokker–Planck solver or Monte Carlo simulations, particularly for the most energetic ions.

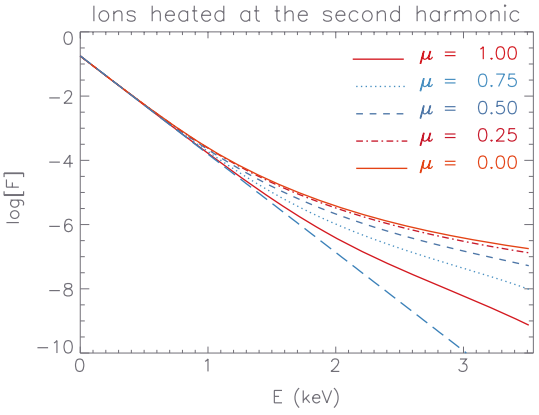

Figure 3. Ion distribution function at $r/a = 0.25$ for a total coupled power of 0.044 MW. The long dashed curve is the unperturbed Maxwellian at this radius and a background temperature of 0.155 keV.

3. Results and discussion

We have used TORIC and SSFPQL to simulate second-harmonic heating of the pure hydrogen plasma of the Aditya tokamak. In this study, the Aditya tokamak was operated at 0.75 T toroidal magnetic field. Second-harmonic cyclotron frequency for ions (24.8 MHz) was considered. Under the present experimental conditions, a typical plasma duration was 60–100 ms with 20–30 ms flat-top, 70–90 kA plasma current, central electron density in the range (1–3) $\times 10^{13}$ cm^{-3} and electron temperature around 250–350 eV. The radio frequency (rf) power was gradually increased upto 80 kW. The detailed description of the rf system and experimental conditions can be found in [3]. In all the cases, the ion temperature equal to half of the electron temperature as generally observed in ohmically heated Aditya plasma [8] is considered. The parameters of the representative shot # 20685 taken for the numerical simulation of fast wave absorption in plasma

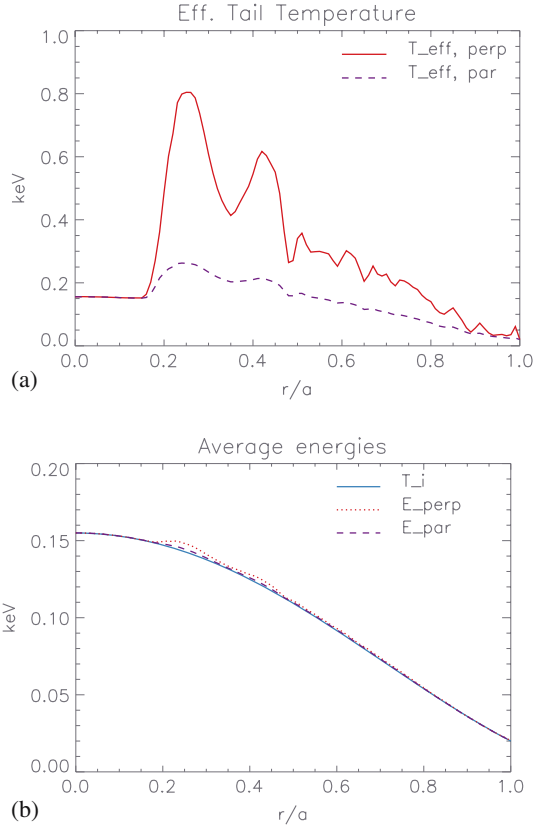

Figure 4. **(a)** Effective perpendicular temperature (solid line, $T_{\text{\_eff, perp}}$) and parallel temperature (dashed line, $T_{\text{\_eff, par}}$) profiles, **(b)** average perpendicular energy (dotted line, $E_{\text{\_perp}}$) and parallel energy (dashed line, $E_{\text{\_par}}$) profiles of hydrogen ions due to the total coupled power of 0.044 MW. The initial ion temperature profile (solid line, T_{i}) is also shown.

are summarized in table 1. The density (n_e) and temperature (T_α) are assumed to have the profiles inside the separatrix:

$$n_e = (n_{e0} - n_{sep})[1 - (r/a)^2] + n_{sep},$$
$$T_\alpha = (T_{\alpha_0} - T_{\alpha sep})[1 - (r/a)^2]^2 + T_{\alpha sep}.$$

Here α = i or e. The subscripts '0' and 'sep' indicate central and separatrix values, respectively.

Figure 1 shows the corresponding power deposition profiles found from TORIC run. These profiles multiplied by the experimentally estimated power of 0.044 MW actually coupled in the experiment are used by SSFPQL.

Power deposition as evaluated from TORIC simulation for shot #20685 is as follows: power deposition on ions from the second-harmonic is ∼35% and is localized mainly at the resonance layer as shown in the poloidal contour plot in figure 2a. Power deposition on electrons is evaluated as ∼65% as shown in figure 2b; the majority of which comes from FW damping on electrons via TTMP, ELD, and their cross-term absorption (direct heating). A small contribution (∼2%) comes from electron Landau damping of ion-Bernstein wave as shown in figure 2c. The TORIC simulation predicts a more central deposition of power for ions around resonance layer, whereas in the case of electrons, deposition is extended to a larger central core region.

Figure 3 is a logarithmic plot of the energy distribution F at constant pitch angle μ derived from quasilinear kinetic equation for ion species at the point of peak hf wave absorption (here peak is at $r/a \approx 0.25 = 6.25$ cm). The calculation is made by assuming a background ion temperature of 0.155 keV, and a power deposition in hydrogen ions of 0.06 W/cm^3 at peak for a total power absorption of 0.044 MW.

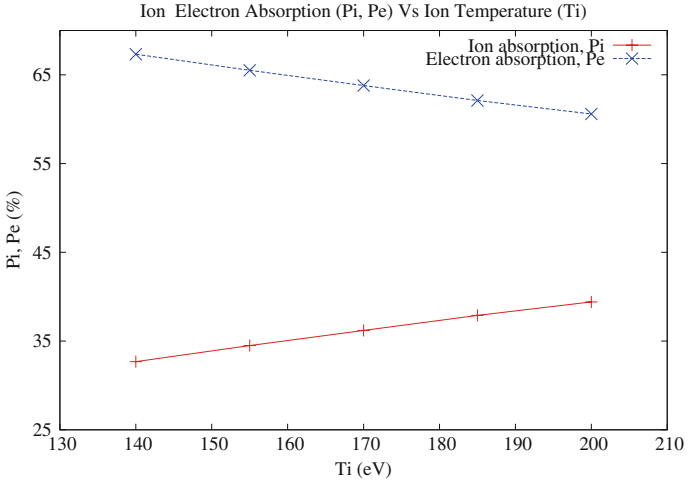

Figure 5. Ion and electron power absorption (in %), P_i and P_e respectively, with ion temperature (T_i).

Figure 4a shows the maximum effective perpendicular ion temperature (logarithmic energy derivation at $v_{\parallel} = 0$ of figure 3) of the tail as ∼0.800 keV, whereas the maximum parallel effective ion temperature of the tail is ∼0.250 keV in steady state due to absorption of rf waves around second-harmonic resonance layer. Increase in perpendicular temperature is less compared to that in high-temperature plasma as observed in ICRH-heated tokamak [6].

Average energy as shown in figure 4b is very small indicating that the contribution of suprathermal hydrogen to the total energy is minimal [6]. This also indicates that the density of suprathermal hydrogen ions is very small. This is expected because it is a well-known fact that harmonic heating is a finite Larmor radius effect and hence will be effective at higher temperature of ions [4,7]. This statement is further verified by our simulation work keeping other plasma parameters constant and is shown in figure 5. The figure shows that the power absorption by ions (P_i) increases (line with '+' in the

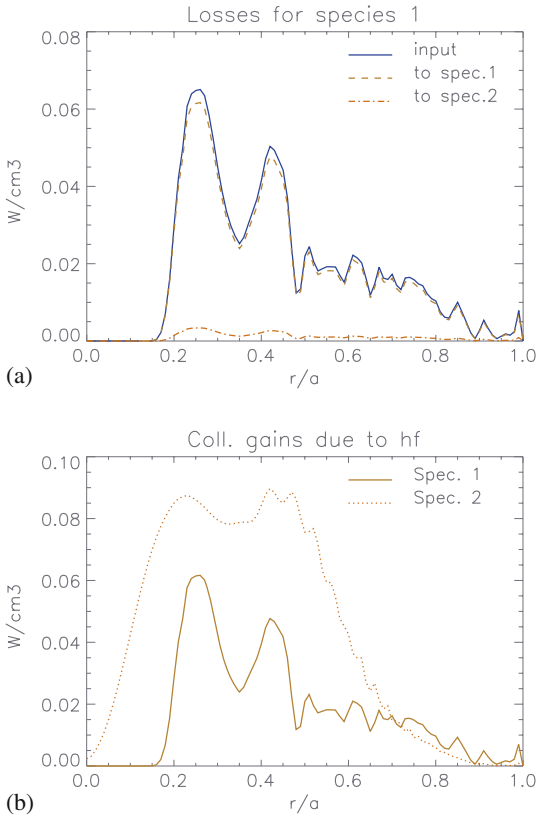

Figure 6. **(a)** Collisional power losses of rf-heated hydrogen ions (solid line, 'input') to the background ion (dashed line, 'to spec. 1') and electrons (dot–dashed line, 'to spec. 2'), **(b)** the power profiles of ions (solid line, 'spec. 1') and electrons (dotted line, 'spec. 2') due to collisional gain.

figure) with the increase in ion temperature (T_i) whereas power absorption by electrons (P_e) decreases (line with 'x' in the figure).

Figure 6a shows the collisional loss of energy of hf wave-heated hydrogen ions (protons) to the background ions and electrons. Most of the power absorbed by the protons from the waves is collisionally transferred to the background ions. A small portion is transferred to background electrons. This phenomenon is generally observed in plasma with moderate effective temperature of suprathermal tail [6]. The power profiles of electrons and ions due to collisional gain are shown in figure 6b.

4. Conclusions

We have presented the second-harmonic ICRF wave absorption scenarios of single ion species Aditya plasma having low density and low temperature with the full wave code TORIC and the quasilinear Fokker–Planck solver SSFPQL. The wave absorption by hydrogen is low which is expected, as the wave absorption at the second-harmonic resonance relies on FLR effect. Therefore, efficiency of this heating scheme depends critically on the ion temperature. Since the ion temperature in Aditya is low for second-harmonic heating, the wave absorption by hydrogen is low. On the other hand, significant amount of direct electron heating is observed in low-temperature Aditya plasma due to second-harmonic heating. It is expected that second-harmonic resonance heating will be more effective in our superconducting tokamak SST-1 [9] due to higher ion temperature. We believe that the numerically found ion temperature will be useful for developing and benchmarking of the charge exchange diagnostic developed for the Aditya tokamak. In the near future, we shall calculate the density of suprathermal hydrogen contributing to the total energy in single-species Aditya plasma.

Acknowledgements

The author (AKC) gratefully acknowledges the procurement of the TORIC ion cyclotron code and the help in understanding the code from Max-Planck Institute for Plasma Physics (IPP), Garching, Germany. The author (AKC) thanks R Ganesh for patiently reading the manuscript and for various fruitful suggestions.

References

[1] M Brambilla, *Kinetic theory of plama waves – Homogeneous plasma* (Oxford University Press Inc, New York, 1998)
[2] S B Bhatt, *Indian J. Pure Appl. Phys.* **27**, 710 (1989)
[3] Kishore Mishra *et al*, *Plasma Phys. Control. Fusion* **53**, 095011 (2011)
[4] M Brambilla, *Plasma Phys. Control. Fusion* **41**, 1 (1999)
[5] M Brambilla, *Nucl. Fusion* **34**, 1121 (1994)
[6] M Brambilla and R Bilato, *Nucl. Fusion* **46**, S387 (2006)
[7] M Brambilla, *Plasma Phys. Control. Fusion* **31**, 723 (1989)
[8] Santosh Pandya, Kumar Ajay, Priyanka Mishra, Rajani Dhingra and J Govindarajan, *Rev. Sci. Instrum.* **84**, 023503 (2013)
[9] Y C Saxena and SST-1 Team, *Nucl. Fusion* **40**, 1069 (2000)